

Exact Smooth Reformulations for Trajectory Optimization Under Signal Temporal Logic Specifications

Shaohang Han, Joris Verhagen, and Jana Tumova

Abstract—We study motion planning under Signal Temporal Logic (STL), a useful formalism for specifying spatial-temporal requirements. We pose STL synthesis as a trajectory optimization problem leveraging the STL robustness semantics. To obtain a differentiable problem without approximation error, we introduce an exact reformulation of the \max and \min operators. The resulting method is exact, smooth, and sound. We validate it in numerical simulations, demonstrating its practical performance.

I. INTRODUCTION

Temporal logics are formal specification languages used to describe complex desired behaviors of autonomous systems. One such language is Signal Temporal Logic (STL) [1], which supports quantitative temporal properties (e.g., the robot should be in region A every 10–20 seconds and in region B every 15–25 seconds). From a motion planning standpoint, STL is particularly appealing because it admits quantitative semantics via the notion of *robustness*. The robustness measures the *degree* to which a trajectory satisfies a given STL specification. Through this unique property, we can formulate an optimization problem to find a maximally robust trajectory that satisfies the STL specification [2]. Therefore, STL trajectory optimization has become an active research topic in robotic applications ranging from mobile robots [3] to manipulators [4], [5] and bipedal robots [6].

The robustness semantics rely on \max and \min operators to capture logical disjunctions, conjunctions, and temporal ambiguity. However, these operators are challenging to embed in optimization problems because they are non-smooth and can be non-convex. A common approach is to encode them using Mixed-Integer Programming (MIP) with the help of binary variables. In particular, mixed-integer convex programming (MICP) formulations [2], [7]–[9] are guaranteed to be complete, sound, and globally optimal for systems with linear dynamics and convex predicates. Despite their effectiveness in this regime, these formulations do not readily extend to problems with nonlinear dynamics or nonlinear predicates. Their combinatorial complexity due to binary variables becomes prohibitive for high-dimensional systems, long planning horizons, or complex formulas.

To circumvent the non-smoothness issue, researchers have also explored sampling-based trajectory optimization meth-

ods, such as Model Predictive Path Integral (MPPI) [10], [11]. This type of method iteratively refines trajectories using estimated gradients computed from random rollouts. However, these estimates can exhibit high variance, which could lead to unstable convergence, making them scale poorly to long horizons.

An alternative is to utilize approximate smooth robustness degree [12]–[15], where the \max and \min operators are replaced by smooth approximations. The resulting smooth functions admit derivatives, making them amenable to Nonlinear Programming (NLP) formulations that can be solved using off-the-shelf derivative-based numerical solvers. Specifically, [12] proposes log-sum-exponential approximations, which are smooth everywhere but not sound. In contrast, [15] introduces arithmetic–geometric mean robustness, which is sound but not smooth everywhere. The authors in [13] propose different approximations that are both sound and smooth. In [13], the robustness degree with the smooth specification is the under-approximation for the true robustness of the original specification.

Such under-approximation, however, may introduce a sub-optimality gap and can shrink the feasible set when robustness is posed as a constraint. Moreover, [13] relies on hyperparameters that trade off approximation accuracy against numerical conditioning, which requires additional tuning effort. Motivated by this, we instead propose *exact* smooth reformulations of the \max and \min operators for STL trajectory optimization that preserve the true robustness while ensuring differentiability. This removes the error in prior smooth approximations and does not require any tuning parameters. While the reformulation introduces additional variables and constraints, we show in our experiments that the computational overhead can be mitigated by effectively warm-starting the solvers.

This paper is inspired by [16], which introduces an exact smooth reformulation for logic-constrained optimization. We adapt and extend these ideas to STL trajectory optimization, covering both Boolean and temporal operators that allow nesting. To summarize, our contributions are:

- An analysis of the smooth approximation in [13], showing that its error cannot be eliminated in general.
- An exact smooth reformulation for STL trajectory optimization that enables derivative-based NLP solvers.
- Empirical validation in simulations, demonstrating efficiency and practicality, along with an open-source codebase for the community.

This work was partially supported by the Wallenberg AI, Autonomous Systems and Software Program (WASP) funded by the Knut and Alice Wallenberg Foundation.

The authors are with the Division of Robotics, Perception and Learning, School of Electrical Engineering and Computer Science, KTH Royal Institute of Technology, Stockholm, Sweden, and are also affiliated with Digital Futures. Email: {shaohang, jorisv, tumova}@kth.se.

II. PRELIMINARIES AND PROBLEM FORMULATION

In this paper, we consider the nonlinear discrete-time system

$$\mathbf{x}_{t+1} = \mathbf{f}(\mathbf{x}_t, \mathbf{u}_t), \quad (1)$$

where $\mathbf{x}_t \in \mathcal{X} \subseteq \mathbb{R}^n$ is the system state and $\mathbf{u}_t \in \mathcal{U} \subseteq \mathbb{R}^m$ is a control input. We assume that the discrete-time dynamics $\mathbf{f} : \mathbb{R}^n \times \mathbb{R}^m \mapsto \mathbb{R}^n$ is smooth in its arguments. In the following, we consider time steps 0 to T with state trajectory $\mathbf{x} := [\mathbf{x}_0, \mathbf{x}_1, \dots, \mathbf{x}_T]^\top \in \mathbb{R}^{n \times (T+1)}$ and input trajectory $\mathbf{u} := [\mathbf{u}_0, \mathbf{u}_1, \dots, \mathbf{u}_T]^\top \in \mathbb{R}^{m \times (T+1)}$.

A. Signal Temporal Logic

We consider time-bounded STL formulas over nonlinear predicates, which can be defined as:

Definition 1 (Time-bounded STL). *Let $I = [t_1, t_2] \subset \mathbb{Z}_{\geq 0}$ be a closed bounded time interval, where $t_1 \leq t_2$. STL formulas can be recursively written as*

$$\varphi ::= \mu \mid \neg\varphi \mid \wedge_i \varphi_i \mid \vee_i \varphi_i \mid \square_I \varphi \mid \diamond_I \varphi \mid \varphi_1 \mathbf{U}_I \varphi_2,$$

where $\mu := h^\mu(\mathbf{x}) \geq 0$ is a predicate with smooth function $h^\mu : \mathcal{X} \mapsto \mathbb{R}$. \neg stands for negation. \wedge and \vee denote Boolean operations “and” and “or”. \square_I and \diamond_I stand for the “always” and “eventually” operators meaning that φ should hold $\forall t \in I$ or $\exists t \in I$ respectively. \mathbf{U}_I represents the “until” operator which specifies φ_1 should hold until, within I , φ_2 should hold.

STL formulas are associated with *quantitative* semantics such as *spatial robustness* [1], which indicates the degree of satisfaction or violation of the specification. The robustness function evaluated at time t for a trajectory \mathbf{x} and formula φ is denoted as $\rho^\varphi(\mathbf{x}, t) \in \mathbb{R}$. If a trajectory \mathbf{x} satisfies the formula φ , we denote that $\mathbf{x} \models \varphi$. The semantics can then be recursively defined as follows:

Definition 2 (STL Robustness Semantics).

$$\begin{aligned} \mathbf{x} \models \varphi &\Leftrightarrow \rho^\varphi(\mathbf{x}, 0) \geq 0 \\ \rho^\mu(\mathbf{x}, t) &= h^\mu(\mathbf{x}_t) \\ \rho^{\neg\varphi}(\mathbf{x}, t) &= -\rho^\varphi(\mathbf{x}, t) \\ \rho^{\varphi_1 \wedge \varphi_2}(\mathbf{x}, t) &= \min([\rho^{\varphi_1}(\mathbf{x}, t), \rho^{\varphi_2}(\mathbf{x}, t)]^\top) \\ \rho^{\varphi_1 \vee \varphi_2}(\mathbf{x}, t) &= \max([\rho^{\varphi_1}(\mathbf{x}, t), \rho^{\varphi_2}(\mathbf{x}, t)]^\top) \\ \rho^{\diamond_I \varphi}(\mathbf{x}, t) &= \max([\rho^\varphi(\mathbf{x}, t')^\top]_{t' \in t+I}) \\ \rho^{\square_I \varphi}(\mathbf{x}, t) &= \min([\rho^\varphi(\mathbf{x}, t')^\top]_{t' \in t+I}) \\ \rho^{\varphi_1 \mathbf{U}_I \varphi_2}(\mathbf{x}, t) &= \max\left(\left[\min([\rho^{\varphi_2}(\mathbf{x}, t'), [\rho^{\varphi_1}(\mathbf{x}, t'')^\top]_{t'' \in [t, t']}]^\top)^\top]_{t' \in t+I} \right)^\top \right). \end{aligned}$$

In the following, we use $\rho^\varphi(\mathbf{x})$ as shorthand for $\rho^\varphi(\mathbf{x}, 0)$.

B. STL Robustness Tree

For discrete-time systems, STL robustness can be parsed using a tree structure as introduced in [7], [17]. In this robustness tree, the leaf nodes store the robustness degree of an atomic predicate at each time step, and an internal node has only max or min type. This differs from the STL syntax

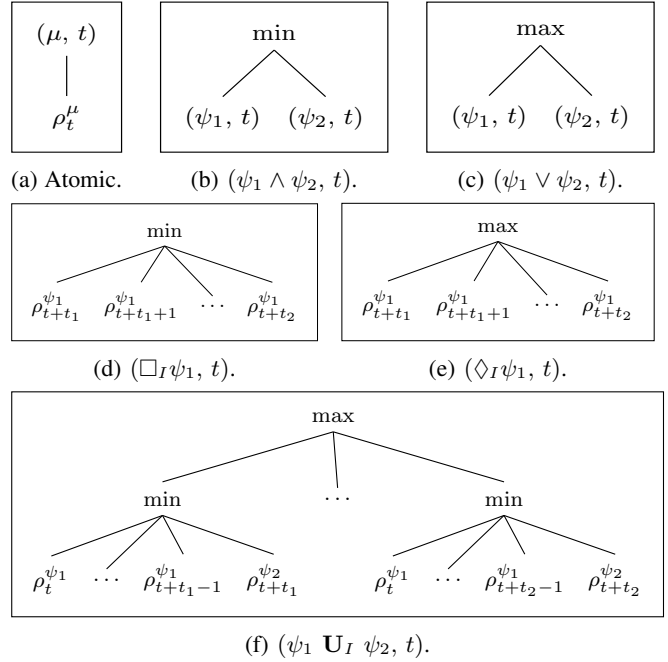


Fig. 1: Building blocks used to construct a robustness tree.

tree used in [18], [19], which contains *set* nodes representing the feasible sets specified by subformulas over time intervals. The STL robustness tree can be formally defined as follows and illustrated in Fig. 1.

Definition 3 (STL Robustness Tree). *The robustness tree \mathcal{T}^φ is a finite rooted, ordered tree whose nodes are labeled by pairs (ψ, t) , where ψ is a subformula of φ and t is a time index. Every internal node is typed as max or min according to the robustness semantics. The tree is constructed recursively:*

- If ψ is an atomic predicate μ , then (μ, t) is a leaf. Its value is the predicate robustness $\rho^\mu(\mathbf{x}, t) \in \mathbb{R}$.
- If $\psi = \psi_1 \wedge \psi_2$, then (ψ, t) is a min-node with two children (ψ_1, t) and (ψ_2, t) .
- If $\psi = \psi_1 \vee \psi_2$, then (ψ, t) is a max-node with two children (ψ_1, t) and (ψ_2, t) .
- If $\psi = \square_I \psi_1$, then (ψ, t) is a min-node with children $\{(\psi_1, t + t')\}_{t' \in I}$.
- If $\psi = \diamond_I \psi_1$, then (ψ, t) is a max-node with children $\{(\psi_1, t + t')\}_{t' \in I}$.
- If $\psi = \psi_1 \mathbf{U}_I \psi_2$, then (ψ, t) is a max-node with one child per $t' \in I$; its t' -th child is a min-node with children $\{(\psi_1, t + j)\}_{j=0}^{t'-1}$ and $(\psi_2, t + t')$.

By traversing the robustness tree in a depth-first order, we can either embed the STL specification into an optimization problem or compute the robustness degree for a given trajectory, as shown in [7].

C. Problem Formulation

Given a nonlinear system (1), an STL specification φ , and an initial state \mathbf{x}_0 , we seek a state trajectory \mathbf{x} and an input trajectory \mathbf{u} that satisfy φ , while optimizing for

a user-defined objective function. Formally, the motion planning problem can be formulated as the following trajectory optimization problem under the STL specification.

Problem 1. Given a nonlinear system (1), an initial state \mathbf{x}_0 , and an STL specification φ , solve

$$\min_{\mathbf{x}, \mathbf{u}} \quad -\alpha \rho^\varphi(\mathbf{x}) + \sum_{t=0}^T \mathbf{x}_t^\top \mathbf{Q} \mathbf{x}_t + \mathbf{u}_t^\top \mathbf{R} \mathbf{u}_t \quad (2a)$$

$$\text{s.t.} \quad \forall t \in [0, T-1] : \mathbf{x}_{t+1} = \mathbf{f}(\mathbf{x}_t, \mathbf{u}_t), \quad (2b)$$

$$\mathbf{x}_0 \text{ fixed}, \quad (2c)$$

$$\forall t \in [0, T] : \mathbf{x}_t \in \mathcal{X}, \quad \mathbf{u}_t \in \mathcal{U}, \quad (2d)$$

$$\rho^\varphi(\mathbf{x}) \geq 0, \quad (2e)$$

where α is a positive weight, $\mathbf{Q} \succeq 0$ and $\mathbf{R} \succeq 0$ are symmetric weighting matrices.

Remark 1. Compared to a standard trajectory optimization problem, (2) augments the objective (2a) with the term $-\alpha \rho^\varphi(\mathbf{x})$ to maximize the degree of STL satisfaction, while also including standard performance terms such as control-effort minimization. When \mathbf{Q} and \mathbf{R} are both $\mathbf{0}$, (2) solves for a maximally robust trajectory. The constraint (2e) is added to enforce satisfaction of the formula.

The function $\rho^\varphi(\mathbf{x})$ is generally non-smooth due to the max/min operators. Smooth under-approximations [13] replace $\rho^\varphi(\mathbf{x})$ with a smooth surrogate $\tilde{\rho}^\varphi(\mathbf{x}) = \rho^\varphi(\mathbf{x}) - \epsilon(\mathbf{x})$, where ϵ denotes the non-negative error. However, this error cannot be computed without using discrete max/min and solving (2). As a result, [13] directly uses $\tilde{\rho}^\varphi$ in (2), which prevents accurately quantifying the optimal spatial robustness in (2a), and can shrink the feasible set by making (2e) more conservative.

In the following, we first provide a quantitative analysis of the smooth approximations in [13] and show that the resulting errors are unavoidable in general. We then present our main results on exact reformulations.

III. ANALYSIS OF THE SMOOTH APPROXIMATIONS

Given a vector $\mathbf{a} = [a_1, \dots, a_m]^\top$, [13] proposes the following under-approximations for max and min operators:

$$\begin{aligned} \widetilde{\max}(\mathbf{a}) &= \frac{\sum_{i=1}^m a_i e^{ka_i}}{\sum_{i=1}^m e^{ka_i}}, \\ \widetilde{\min}(\mathbf{a}) &= -\frac{1}{k} \log \left(\sum_{i=1}^m e^{-ka_i} \right), \end{aligned} \quad (3)$$

where $k > 0$. These approximations are widely used due to their soundness and practical simplicity [4], [20]. The authors in [13], [14] also provide the upper bounds of the resulting approximation errors. Instead, in the following lemma, we establish lower bounds on the approximation errors.

Lemma 1. Given $k > 0$ and a vector $\mathbf{a} = [a_1, \dots, a_m]^\top$. Without loss of generality, we may assume that $m \geq 2$ and \mathbf{a} is ordered so that $a_1 \geq \dots \geq a_m$, since max, min and (3) are invariant under permutations of the entries. Let r be the number of entries attaining the maximum (i.e.,

$a_1 = \dots = a_r > a_{r+1}$) and let s be the number of entries attaining the minimum (i.e., $a_{m-s} > a_{m-s+1} = \dots = a_m$). Let $w_i := \frac{e^{ka_i}}{\sum_{j=1}^m e^{ka_j}}$. Then

$$\begin{aligned} \Delta_{\max} &= \max(\mathbf{a}) - \widetilde{\max}(\mathbf{a}) \geq (a_1 - a_{r+1}) \sum_{i=r+1}^m w_i, \\ \Delta_{\min} &= \min(\mathbf{a}) - \widetilde{\min}(\mathbf{a}) \geq \frac{1}{k} \log \left(s + \sum_{i=1}^{m-s} e^{-k(a_i - a_m)} \right). \end{aligned}$$

Proof. For the maximum, the error is

$$\begin{aligned} \Delta_{\max} &= a_1 - \sum_{i=1}^m w_i a_i = \sum_{i=1}^m w_i (a_1 - a_i) \\ &= \sum_{i=r+1}^m w_i (a_1 - a_i) \geq (a_1 - a_{r+1}) \sum_{i=r+1}^m w_i. \end{aligned}$$

For the minimum, the error is

$$\begin{aligned} \Delta_{\min} &= a_m + \frac{1}{k} \log \sum_{i=1}^m e^{-ka_i} = \frac{1}{k} \log \left(e^{ka_m} \sum_{i=1}^m e^{-ka_i} \right) \\ &= \frac{1}{k} \log \sum_{i=1}^m e^{-k(a_i - a_m)} \\ &\geq \frac{1}{k} \log \left(s + \sum_{i=1}^{m-s} e^{-k(a_i - a_m)} \right), \end{aligned}$$

which completes the claim. \square

By inspecting Lemma 1, we can tell that $\Delta_{\max} > 0$ whenever \mathbf{a} contains an a_{r+1} that is smaller than a_1 . $\Delta_{\min} > 0$ always holds under the assumption $m \geq 2$. Since the error ϵ is obtained by recursively combining Δ_{\max} and Δ_{\min} , as demonstrated in [13], it cannot be eliminated in general. One way to mitigate the approximation error is to tune the parameter k . However, a large k makes the exponentials grow rapidly, leading to numerical instability, whereas a small k could increase the error.

IV. EXACT SMOOTH REFORMULATION

Motivated by the shortcomings of (3), we propose exact, smooth reformulations of the max and min operators. We then recursively apply these rules to the STL robustness trees to reformulate the optimization problem in (2).

A. Node-wise Reformulation Rules

For any finite index set \mathcal{J} and real-valued functions $\{\rho_j\}_{j \in \mathcal{J}}$, we write $\min_{j \in \mathcal{J}} \rho_j$ and $\max_{j \in \mathcal{J}} \rho_j$ for pointwise minimum and maximum. We also introduce a continuous variable $\delta \in \mathbb{R}$ to present the following lemmas.

Lemma 2. Let $\{\rho_j\}_{j \in \mathcal{J}}$ be finite. Then

$$\min_{j \in \mathcal{J}} \rho_j(\mathbf{x}) \geq \delta \iff \rho_j(\mathbf{x}) \geq \delta \quad \forall j \in \mathcal{J}.$$

Lemma 3. Let $\{\rho_j\}_{j \in \mathcal{J}}$ be finite. Then

$$\max_{j \in \mathcal{J}} \rho_j(\mathbf{x}) \geq \delta \iff \exists \boldsymbol{\lambda} \in \mathbb{S}^{|\mathcal{J}|} : \sum_{j \in \mathcal{J}} \lambda_j \rho_j(\mathbf{x}) \geq \delta,$$

Algorithm 1 Depth-First Traversal

Require: Robustness tree \mathcal{T}^φ **Ensure:** Constraints \mathcal{C} ; auxiliary variables \mathcal{V}_ρ and \mathcal{V}_λ ; root robustness variable ρ_r

```
1:  $\mathcal{C} \leftarrow \emptyset$ ,  $\mathcal{V}_\rho \leftarrow \emptyset$ ,  $\mathcal{V}_\lambda \leftarrow \emptyset$ 
2: function TRAVERSE( $v$ ) ▷  $v = (\psi, t)$ 
3:   create scalar variable  $\rho_v$ ; add  $\rho_v$  to  $\mathcal{V}_\rho$ 
4:   if  $v$  is leaf  $(\mu, t)$  then
5:     add  $h^\mu(\mathbf{x}_t) \geq \rho_v$  to  $\mathcal{C}$ 
6:   else if  $v$  is min-node then ▷ Lemma 2
7:     for all  $u \in \text{ch}(v)$  do
8:        $\rho_u \leftarrow \text{TRAVERSE}(u)$ 
9:       add  $\rho_u \geq \rho_v$  to  $\mathcal{C}$ 
10:  else if  $v$  is max-node then ▷ Lemma 3
11:    let  $\{u_j\}_{j=1}^m \leftarrow \text{ch}(v)$ 
12:    for  $j = 1$  to  $m$  do
13:       $\rho_{u_j} \leftarrow \text{TRAVERSE}(u_j)$ 
14:    create  $\boldsymbol{\lambda}^v \in \mathbb{R}^m$ ; add  $\boldsymbol{\lambda}^v$  to  $\mathcal{V}_\lambda$ 
15:    add  $\boldsymbol{\lambda}^v \geq 0$  and  $\mathbf{1}^\top \boldsymbol{\lambda}^v = 1$  to  $\mathcal{C}$ 
16:    add  $\sum_{j=1}^m \lambda_j^v \rho_{u_j} \geq \rho_v$  to  $\mathcal{C}$ 
17:  return  $\rho_v$ 
18:  $\rho_r \leftarrow \text{TRAVERSE}(\text{root})$ 
19: add  $\rho_r \geq 0$  to  $\mathcal{C}$ 
20: return  $(\mathcal{C}, \mathcal{V}_\rho, \mathcal{V}_\lambda, \rho_r)$ 
```

where $\mathbb{S}^{|\mathcal{J}|} = \{\boldsymbol{\lambda} \in \mathbb{R}^{|\mathcal{J}|} \mid \boldsymbol{\lambda} \geq 0, \mathbf{1}^\top \boldsymbol{\lambda} = 1\}$.

Proof. Let $j^* \in \arg \max_j \rho_j(\mathbf{x})$. (\Rightarrow) Setting $\lambda_{j^*} = 1$ and $\lambda_j = 0$ for $j \neq j^*$, then $\sum_j \lambda_j \rho_j = \rho_{j^*} \geq \delta$. (\Leftarrow) Since $\sum_j \lambda_j = 1$, we have $\rho_{j^*} = \sum_j \lambda_j \rho_{j^*} \geq \sum_j \lambda_j \rho_j$. Therefore, $\max_j \rho_j = \rho_{j^*} \geq \delta$. \square

B. Recursive Reformulation on the Robustness Tree

We reformulate the STL specification in (2) as a collection of smooth constraints with auxiliary variables. The procedure is summarized in Algorithm 1. In this algorithm, we traverse the robustness tree \mathcal{T}^φ in depth-first order. At leaf nodes, we encode the robustness using predicate functions (lines 4-5); at internal nodes, we apply Lemmas 2 and 3 node-wise (lines 6-16). We denote by \mathcal{V}_ρ and \mathcal{V}_λ the collections of auxiliary variables introduced by the traversal, and by \mathcal{C} the collection of all resulting constraints. The next lemma shows that this reformulation preserves the feasible set.

Lemma 4. Let $\mathcal{F}_{\text{org}} := \{\mathbf{x} \mid \rho^\varphi(\mathbf{x}) \geq 0\}$ be the original feasible set, and let \mathcal{C} be the collection of constraints returned by Algorithm 1. We can define

$$\mathcal{F}_{\text{new}} = \left\{ \mathbf{x} \mid \exists (\mathcal{V}_\rho, \mathcal{V}_\lambda, \rho_r) \text{ such that } (\mathbf{x}, \mathcal{V}_\rho, \mathcal{V}_\lambda, \rho_r) \text{ satisfy } \mathcal{C} \right\}.$$

Then $\mathcal{F}_{\text{new}} = \mathcal{F}_{\text{org}}$.

Proof. By construction, the constraints \mathcal{C} implement the semantics of ρ^φ . If $\mathbf{x} \in \mathcal{F}_{\text{org}}$, by Lemma 2 and 3, there exist $(\mathcal{V}_\rho, \mathcal{V}_\lambda, \rho_r)$ satisfying \mathcal{C} , hence $\mathbf{x} \in \mathcal{F}_{\text{new}}$. Conversely,

if $\mathbf{x} \in \mathcal{F}_{\text{new}}$, there exist $(\mathcal{V}_\rho, \mathcal{V}_\lambda, \rho_r)$ such that $(\mathbf{x}, \mathcal{V}_\rho, \mathcal{V}_\lambda, \rho_r)$ satisfy \mathcal{C} with $\rho_r \geq 0$, which implies $\mathbf{x} \in \mathcal{F}_{\text{org}}$. \square

Theorem 1 (Soundness). *For any discrete-time trajectory \mathbf{x} and time-bounded STL formula φ , if there exist $(\mathcal{V}_\rho, \mathcal{V}_\lambda, \rho_r)$ such that the constraint set \mathcal{C} is satisfied, then \mathbf{x} satisfies the specification, i.e. $\mathbf{x} \models \varphi$.*

Proof. By Lemma 4, feasibility of $(\mathbf{x}, \mathcal{V}_\rho, \mathcal{V}_\lambda, \rho_r)$ with $\rho_r \geq 0$ implies $\rho^\varphi(\mathbf{x}) \geq 0$, hence $\mathbf{x} \models \varphi$. \square

For a node with m children, Algorithm 1 introduces $O(m)$ auxiliary variables for a min-node and $O(2m)$ for a max-node, so the total number of added variables and constraints grows linearly with the size of the robustness tree, thus polynomially in the STL formula size. Compared to [13], our method adds m more $\boldsymbol{\lambda}$ -variables at each max-node, but the reformulated problem remains smooth and preserves the original feasible set. In the experiments, we show that our method has comparable running time to [13] in most cases, while yielding better optimal values.

As every min/max operator introduces auxiliary variables, the form in which the formula is presented to Algorithm 1 impacts the efficiency of the embedding. As such, we apply the formula flattening technique from [7] to simplify the robustness trees. It recursively removes consecutive internal nodes of the same type while maintaining equivalence of the STL formula.

C. Final Smooth NLP

The final reformulated smooth NLP is given by:

$$\begin{aligned} \min_{\mathbf{x}, \mathbf{u}, \mathcal{V}_\rho, \mathcal{V}_\lambda, \rho_r} \quad & -\alpha \rho_r + \sum_{t=0}^T \mathbf{x}_t^\top \mathbf{Q} \mathbf{x}_t + \mathbf{u}_t^\top \mathbf{R} \mathbf{u}_t \\ \text{s.t.} \quad & \forall t \in [0, T-1] : \mathbf{x}_{t+1} = \mathbf{f}(\mathbf{x}_t, \mathbf{u}_t), \\ & \mathbf{x}_0 \text{ fixed}, \\ & \forall t \in [0, T] : \mathbf{x}_t \in \mathcal{X}, \mathbf{u}_t \in \mathcal{U}, \\ & (\mathbf{x}, \mathcal{V}_\rho, \mathcal{V}_\lambda, \rho_r) \text{ satisfy all constraints in } \mathcal{C}. \end{aligned} \quad (4)$$

Here \mathbf{x}, \mathbf{u} are the original decision variables, and $(\mathcal{V}_\rho, \mathcal{V}_\lambda, \rho_r)$ are auxiliary decision variables introduced by the exact smooth reformulation.

Corollary 1. *The reformulated problem (4) has the same global optimal value as the original problem (2).*

Proof. By Lemma 4, the feasible sets are identical. Since the objective function is unchanged, the global optimal values coincide. \square

Remark 2. *From an optimization standpoint, we do not show that the reformulation preserves the correspondence of the global minimizer. Thus, although Corollary 1 ensures that the optimal values coincide, we do not formally guarantee that a numerical solver will find it.*

A possible route to certify the correspondence of minimizer is to convert the formulas to conjunctive normal form (CNF) and encode them as max-min constraints [16], [21]. However, this transformation increases formula size

and, in turn, the runtime of nonlinear numerical solvers. Instead, our experiments indicate that our direct reformulation works well with off-the-shelf smooth NLP solvers and consistently yields trajectories with lower optimal values than the approximation-based baseline [13]. Moreover, with good warm starts, we often observe convergence to the global optimum, as shown in Section V-A.

To warm-start $(\mathcal{V}_\rho, \mathcal{V}_\lambda, \rho_r)$ given a reference trajectory \mathbf{x}_{ref} , we traverse \mathcal{T}^φ , similar to Algorithm 1. For each node v , we evaluate robustness on \mathbf{x}_{ref} using the discrete max and min, and record ρ_v (with ρ_r at the root). Since λ is only introduced for max operators, for each max-node v with children $\text{ch}(v) = \{u_j\}_{j=1}^m$, we set $j^* = \arg \max_j \rho_{u_j}$, then define $\lambda^v \in \mathbb{R}^m$ by $\lambda_{j^*}^v = 1$ and $\lambda_j^v = 0$ for $j \neq j^*$. Lastly, we store ρ_v in \mathcal{V}_ρ and λ^v in \mathcal{V}_λ .

V. NUMERICAL EXPERIMENTS

We validate the proposed method in both linear benchmarks and a nonlinear case study, all involving a mobile robot navigating in planar environments. Our Python implementation¹ builds on the code in [7] and uses Drake’s [22] mathematical programming interface. We use SNOPT [23], a Sequential Quadratic Programming (SQP) solver, to solve the NLPs. All experiments were run on a laptop with an Intel Core i7-13700H CPU and 32 GB RAM.

A. Linear Benchmarks

We benchmark on the linear-dynamics, linear-predicate scenarios from [7]. The robot follows discrete-time double-integrator dynamics

$$\mathbf{x}_t = [p_{x_t}, p_{y_t}, \dot{p}_{x_t}, \dot{p}_{y_t}]^\top \in \mathbb{R}^4, \quad \mathbf{u}_t = [\ddot{p}_{x_t}, \ddot{p}_{y_t}]^\top \in \mathbb{R}^2,$$

where p_{x_t} and p_{y_t} are the horizontal and vertical positions. The dynamics are

$$\mathbf{x}_{t+1} = \mathbf{A}\mathbf{x}_t + \mathbf{B}\mathbf{u}_t, \quad \mathbf{A} = \begin{bmatrix} \mathbf{I}_2 & \mathbf{I}_2 \\ \mathbf{0} & \mathbf{I}_2 \end{bmatrix}, \quad \mathbf{B} = \begin{bmatrix} \mathbf{0} \\ \mathbf{I}_2 \end{bmatrix},$$

where \mathbf{I}_2 and $\mathbf{0}$ are the 2×2 identity and zero matrices, respectively. We use the initial states from [7], set $\alpha = 1$, $\mathbf{Q} = \text{diag}(0, 0, 1, 1)$, $\mathbf{R} = \mathbf{I}_2$, and vary the time horizon T .

We compare our method to the NLP using smooth approximations [13] and the MICP formulation [2]. To warm-start the NLPs across different time horizons, we linearly interpolate the MICP solutions computed at $T = 25$. For [13], we use grid search to find the parameter k that minimizes the optimal value. We use Gurobi [24] to solve the MICPs. The wall-clock solve time is capped at 600 s. Runs exceeding this limit are reported as timeouts.

Table I reports the optimal values and solve times. MICP is guaranteed to find the global optimal solutions, but it can easily run into a timeout due to the combinatorial complexity. Instead, both NLP-based methods are more scalable than MICP. Among them, our method consistently attains better optimal values than [13]. At $T = 25$, we warm-start both NLP-based methods with the globally optimal

TABLE I: Results of linear scenarios. (-) indicates a timeout.

Scenario	T	Optimal Value ↓			Solve Time (s) ↓		
		MICP	Ours	[13]	MICP	Ours	[13]
Two-Target	25	3.94	3.94	4.00	0.39	0.01	0.66
	50	1.67	1.68	1.70	469.52	5.14	5.24
	75	-	0.96	0.98	-	11.56	10.35
Many-Target	25	6.94	6.94	7.08	2.39	0.01	1.21
	50	-	3.32	3.37	-	9.79	8.10
	75	-	2.18	2.22	-	35.55	21.54
Narrow-Passage	25	1.83	1.83	1.89	1.30	0.01	0.30
	50	0.88	0.88	0.92	82.22	8.70	2.70
	75	-	0.53	0.58	-	32.89	8.09
Door-Puzzle	25	27.69	27.69	30.10	3.68	0.03	0.97
	50	-	12.58	14.00	-	568.83	9.62
	75	-	-	8.86	-	-	47.50

MICP solutions. Interestingly, our method preserves these optimal values, whereas [13] often degrades due to the approximation error. For $T > 25$, the optimal values of our method can underperform MICP. This is because our method is always warm-started from the $T = 25$ MICP solutions via interpolation, which are no longer optimal with a larger T . Regarding runtime, our method is very fast when the initial guesses are good. However, this speed advantage does not always persist. While customizing solvers may further improve the speed, it is beyond the scope of this paper.

B. Nonlinear Case Study

We then validate the proposed method on a scenario with nonlinear dynamics and nonlinear predicates. The state and control input are defined as

$$\mathbf{x}_t = [p_{x_t}, p_{y_t}, \theta_t]^\top \in \mathbb{R}^3, \quad \mathbf{u}_t = [v_t, \omega_t]^\top \in \mathbb{R}^2,$$

where p_{x_t} and p_{y_t} denote the robot’s horizontal and vertical positions, and θ_t is the heading. The system follows a kinematic unicycle model,

$$\mathbf{x}_{t+1} = \mathbf{f}(\mathbf{x}_t, \mathbf{u}_t) = \begin{bmatrix} p_{x_t} + \Delta t v_t \cos \theta_t \\ p_{y_t} + \Delta t v_t \sin \theta_t \\ \theta_t + \Delta t \omega_t \end{bmatrix},$$

where $\Delta t = 0.5$ is the sampling time. We set the time horizon $T = 50$, and the STL specification is defined as:

$$\varphi = \square_{[0,2]} \diamond_{[5,7]} \mu_1 \wedge \diamond_{[15,17]} \square_{[2,5]} \mu_2 \\ \wedge \diamond_{[27,35]} (\mu_3 \mathbf{U}_{[2,10]} \mu_1) \wedge \square_{[0,50]} \neg \mu_4 \wedge \diamond_{[37,50]} \mu_5,$$

and $h^{\mu_i} = r_i^2 - (p_{x_t} - c_{i,x})^2 - (p_{y_t} - c_{i,y})^2$, where r_i and $[c_{i,x}, c_{i,y}]^\top$ are the radius and center. We note that this specification cannot be solved by the convex-concave procedure (CCP)-based method in [17] since it requires predicate functions to be convex when the parent node is of type max. Instead, our formulation has no such restriction.

For general nonlinear settings, it is non-trivial to find effective initializations for the NLPs. We therefore use randomized initial guesses drawn from a normal distribution. We set $\alpha = 10$, $\mathbf{Q} = \text{diag}(0, 0, 0)$, and $\mathbf{R} = \text{diag}(0.1, 1)$, and constrain the control inputs by $|v_t| \leq 1$ and $|\omega_t| \leq 1$. The

¹Code available at: https://github.com/KTH-RPL-Planiacs/stl_smooth_reformulation

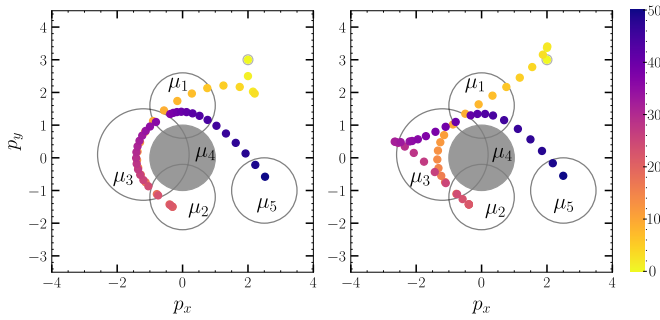


Fig. 2: Comparison of trajectories generated by the baseline method [13] (left) and our approach (right). The color bar indicates the time steps along each trajectory.

initial state $\mathbf{x}_0 = [2, 3, -\pi/2]^\top$. We compare our method with [13] over 100 random seeds. We pick $k = 25$ for the baseline method. The trajectory achieving the lowest objective value is shown in Fig. 2, and corresponding metrics are summarized in Table II.

From the results, we can observe that our method is able to attain a better optimal value, but exhibits a slightly higher infeasibility rate. This may be mitigated with improved initializations. We leave the development of systematic initialization strategies for future work.

TABLE II: Results of the nonlinear scenario. The robustness is computed using the discrete max and min, and infeasible indicates the solver failed to find a solution given a random initial guess.

Method	Optimal Value	Robustness \uparrow	Solve Time (s)	Infeasible
Ours	-1.65	0.80	3.17	19/100
[13]	-0.86	0.79	11.03	14/100

VI. CONCLUSION

In this paper, we take a further step in STL trajectory optimization by providing exact smooth reformulations of the max and min operators. Our approach accommodates general nonlinear dynamics and nonlinear predicates while being exact in quantifying the robustness. We validate the method on linear benchmarks and a nonlinear example. Future work will explore informed warm-start techniques for the NLPs.

ACKNOWLEDGEMENTS

We thank Luyao Zhang, Chelsea Sidrane, and Luzia Knoedler for the helpful discussions.

REFERENCES

- [1] O. Maler and D. Nickovic, "Monitoring temporal properties of continuous signals," in *International symposium on formal techniques in real-time and fault-tolerant systems*. Springer, 2004, pp. 152–166.
- [2] C. Belta and S. Sadraddini, "Formal methods for control synthesis: An optimization perspective," *Annual Review of Control, Robotics, and Autonomous Systems*, vol. 2, no. 1, pp. 115–140, 2019.
- [3] J. Verhagen and J. Tumova, "Collaborative object transportation in space via impact interactions," *arXiv preprint arXiv:2504.18667*, 2025.

- [4] V. Kurtz and H. Lin, "Trajectory optimization for high-dimensional nonlinear systems under stl specifications," *IEEE Control Systems Letters*, vol. 5, no. 4, pp. 1429–1434, 2020.
- [5] R. Takano, H. Oyama, and M. Yamakita, "Continuous optimization-based task and motion planning with signal temporal logic specifications for sequential manipulation," in *IEEE International Conference on Robotics and Automation (ICRA)*, 2021, pp. 8409–8415.
- [6] Z. Gu, Y. Zhao, Y. Chen, R. Guo, J. K. Leestma, G. S. Sawicki, and Y. Zhao, "Robust-locomotion-by-logic: Perturbation-resilient bipedal locomotion via signal temporal logic guided model predictive control," *IEEE Transactions on Robotics*, 2025.
- [7] V. Kurtz and H. Lin, "Mixed-integer programming for signal temporal logic with fewer binary variables," *IEEE Control Systems Letters*, vol. 6, pp. 2635–2640, 2022.
- [8] V. Raman, A. Donzé, M. Maasoumy, R. M. Murray, A. Sangiovanni-Vincentelli, and S. A. Seshia, "Model predictive control with signal temporal logic specifications," in *IEEE Conference on Decision and Control (CDC)*, 2014, pp. 81–87.
- [9] J. Verhagen, L. Lindemann, and J. Tumova, "Temporally robust multi-agent stl motion planning in continuous time," in *IEEE American Control Conference (ACC)*, 2024, pp. 251–258.
- [10] P. Varnai and D. V. Dimarogonas, "The two-stage pi 2 control strategy," *IEEE Control Systems Letters*, vol. 6, pp. 2072–2077, 2021.
- [11] P. Halder, H. Homburger, L. Kiltz, J. Reuter, and M. Althoff, "Trajectory planning with signal temporal logic costs using deterministic path integral optimization," in *IEEE International Conference on Robotics and Automation (ICRA)*, 2025, pp. 4221–4228.
- [12] Y. V. Pant, H. Abbas, and R. Mangharam, "Smooth operator: Control using the smooth robustness of temporal logic," in *IEEE Conference on Control Technology and Applications (CCTA)*, 2017, pp. 1235–1240.
- [13] Y. Gilpin, V. Kurtz, and H. Lin, "A smooth robustness measure of signal temporal logic for symbolic control," *IEEE Control Systems Letters*, vol. 5, no. 1, pp. 241–246, 2020.
- [14] S. Welikala, H. Lin, and P. J. Antsaklis, "Smooth robustness measures for symbolic control via signal temporal logic," *arXiv preprint arXiv:2305.09116*, 2023.
- [15] N. Mehdipour, C.-I. Vasile, and C. Belta, "Arithmetic-geometric mean robustness for control from signal temporal logic specifications," in *IEEE American Control Conference (ACC)*, 2019, pp. 1690–1695.
- [16] J. Wehbeh and E. C. Kerrigan, "Smooth logic constraints in non-linear optimization and optimal control problems," *arXiv preprint arXiv:2506.01742*, 2025.
- [17] Y. Takayama, K. Hashimoto, and T. Ohtsuka, "Stlccp: Efficient convex optimization-based framework for signal temporal logic specifications," *IEEE Transactions on Automatic Control*, 2025.
- [18] C.-I. Vasile, V. Raman, and S. Karaman, "Sampling-based synthesis of maximally-satisfying controllers for temporal logic specifications," in *IEEE/RSJ International Conference on Intelligent Robots and Systems (IROS)*, 2017, pp. 3840–3847.
- [19] P. Yu, X. Tan, and D. V. Dimarogonas, "Continuous-time control synthesis under nested signal temporal logic specifications," *IEEE Transactions on Robotics*, vol. 40, pp. 2272–2286, 2024.
- [20] M. Vahs, C. Pek, and J. Tumova, "Risk-aware spatio-temporal logic planning in gaussian belief spaces," in *IEEE International Conference on Robotics and Automation (ICRA)*, 2023, pp. 7879–7885.
- [21] C. Kirjner-Neto and E. Polak, "On the conversion of optimization problems with max-min constraints to standard optimization problems," *SIAM Journal on Optimization*, vol. 8, no. 4, pp. 887–915, 1998.
- [22] R. Tedrake *et al.*, "Drake: Model-based design and verification for robotics," 2019.
- [23] P. E. Gill, W. Murray, and M. A. Saunders, "Snopt: An sqp algorithm for large-scale constrained optimization," *SIAM review*, vol. 47, no. 1, pp. 99–131, 2005.
- [24] Gurobi Optimization, LLC, "Gurobi Optimizer Reference Manual," 2024. [Online]. Available: <https://www.gurobi.com>